International Journal on Recent and Innovation Trends in Computing and Communication
ISSN: 2321-8169 Volume: 11 Issue: 7
Article Received: *12 May 2023* ***Revised:*** *22 June 2023* ***Accepted:*** *20 July 2023*

Analysis of Induction Motor Drive Systems

Martand Pratap, Dr. Shweta Singh,
Research Scholar, School of Engineering and Technology, MUIT, Lucknow

ABSTRACT

In industry, the induction machine, particularly the cage rotor type, is most typically employed for variable speed applications. Adjustable speed drives use back-to-back AC to DC and DC to AC conversion to alter the speed. This conversion procedure introduces harmonics and reduces power factor at the supply end. It is now more important than ever to design and build a three-phase induction motor drive with higher power quality. A full report on the converter topologies is used for Power Factor Correction at the input side to eliminate harmonics and enhance power factor at the supply side. So the main aim of this study is to improving power quality by raising power factor at input side of an electric drive, hence lowering losses and boosting efficiency.

Keywords: AC to DC and DC to AC conversion, electric drive, power factor, induction motor etc.

INTRODUCTION

Electric drives are currently replacing electrical motors at a rate of 15% each year in an industrialised country. More than 20% of the drives are frequency regulated, whereas the other 80% are constant speed. For varied uses, all industrial, commercial, and other units rely on electrical motors. According to Electric Power Research Institute (EPRI), motors use 51 percent of total global energy consumption. Some industries require far less energy. Lighting, for example, contributes for 19%, heating and cooling systems account for 16%, and information technology accounts for 14%. Therefore, there is a need for an efficient & durable controller for motor control, which will result in energy savings.

Electric motors have an impact on practically every element of modern life. Electric motors are used in refrigerators, vacuum cleaners, elevators, air conditioners, washing machines, fans, computer hard disc drives, & industrial operations. In reality, motors consume majority of energy, regardless of whether application is domestic, industrial, or commercial. The energy percent efficiency of a motor is determined by its kind. Some are designed to be more energy efficient than others. In addition, the recent fast growth of motor drives in vehicle sector with the introduction of new hybrid technologies has produced a significant need for highly efficient variable speed motor drives.

Induction motors are the industry's true workhorses. Because of their inexpensive cost, sturdy construction, and simple control gear, squirrel cage induction motors are employed in the majority of constant speed applications. When one or more of the following considerations are complicated, a wound rotor induction motor is utilised.

1. High starting torque
2. Low starting current
3. Speed control over a limited range

In case of a constant speed application Everyone can benefit from a synchronous motor. Many adjustable speed drives require accurate and continuous speed control with long-term stability, high transient performance, and improved efficiency. Traditional DC motors are easy to build, have a high linear torque-speed characteristic, and are efficient, but they require periodic maintenance and replacement due to the existence of a commutator and brushes. This restricts the use of direct current motors in commercial applications. Moreover, the supplied torque to motor size ratio is weak, limiting its use in areas where space and weight are critical, particularly in electric cars & aerospace applications. As a result, Brushless DC (BLDC) motors have emerged as a superior alternative to traditional DC motors.

Electrical drives are used in both residential and industrial applications every day. Because of the world's energy problem, researchers have been pressed to build an efficient loss-less electric powertrain. The goal of this thesis is to create an energy-efficient electric drive for low-power applications. Induction motor drives are studied and evaluated in the research.

OBJECTIVES OF THE STUDY

- The main aim of this study is improving power quality by raising power factor at input side of an electric drive, hence lowering losses and boosting efficiency.

International Journal on Recent and Innovation Trends in Computing and Communication
ISSN: 2321-8169 Volume: 11 Issue: 7
***Article Received:** 12 May 2023 **Revised:** 22 June 2023 **Accepted:** 20 July 2023*

LITERATURE REVIEW

Rahimi and Emadi (2010) showed the DCM operation of CPL-powered DC/DC converters. If the converter has a resistive load, nonlinear equation of output voltage is obtained using state-space averaging, circuit averaging, or the average-switch technique. The converter's small-signal control-to-output transfer function is then generated using standard linearization methods, and its stability with the resistive load is evaluated in s-domain. The stability of open-loop converter in the s-domain after being loaded by a CPL was then studied.

Rockhill et al. (2011) discussed design process & performance of an LCL grid filter for a medium-voltage neutral point clamped (NPC) converter intended for usage in a multi-megawatt wind turbine. The incorporation of medium voltage converter, a lower allowable switching frequency, considerations about physical size & weight of the component, & severe limits on acceptable injected current harmonics all provide challenges to particular filter design difficulties in this application. A multi-megawatt filter that links a low-frequency switching medium-voltage converter to the electric grid does not follow grid filter design processes for lower power & higher switching frequency converters. This research shows how to use a frequency domain model-based method to find optimal filter settings that deliver desired performance in all operating conditions while sticking to design limitations. New conceptions such as virtual harmonic content & virtual filter losses were introduced to attain this objective.

Errabelli and Mutschler (2012) presented atwo-level fault-tolerant voltage source inverter (VSI) for permanent magnet drives, which was built & tested methodically. A typical two-level inverter has 3-legs. In the case of a fault-tolerant inverter, are dundant leg is added to replace faulty leg. The usage of separate back-to-back-connected thyristors is used to perform faulty leg separation and redundant leg insertion. The suggested inverter can tolerate switching device short-circuit & open-circuit failures. The post-fault performance is comparable to the ordinary pre-fault operation, & fault compensation is sufficiently fast to cause very little distortion in the drive operation. The inverter's fault tolerance is then confirmed using field-oriented control of a permanent magnet synchronous motor.

Lodhi and Thakur (2013) devised an accurate method for 3-phase induction motor speed control. The Indirect Vector Control Induction Motor Drive (IVCIMD) is designed to offer rapid torque and strong dynamic reactions near zero and high speeds. In this study, several controllers are employed to improve performance of indirect vector control, and comparative performance is provided and studied.

Behera et al. (2014) conducted a comparison study of traditional scalar control closed loop v/f control & Indirect Field Oriented Vector Control (IFOC). The PI controller is utilised in both scalar and vector control of induction motors, and it decreases steady-state error while providing smooth tracking. Uncertainties in the system are impacted by unpredictability in machine parameters and external load disruptions. Several robust control approaches, such as optimum control, variable structure control, adaptive fuzzy & neural control, can be used in place of the PI controller.

Ashmore et al. (2015) developed a solar support assembly in which the horizontal frame is coupled to a single pivotal point, resulting in inclination (sag) of the horizontal frame on both frame ends. As a result of the Center's sole support, the seasonal drive arrangement may not operate effectively.

Alexander S. Maklakov et al. (2016) used an 18-pulse connection circuit to create 3 level neutral point clamped (3L-NPC) Active Front-End (AFE) rectifiers for AC drives. Three power transformers are linked in parallel in the circuit, and the secondary winding voltages phase shift. For managing 3L-NPC AFE rectifiers, the authors presented a Pulse Width Modulation Selective Harmonic Elimination (PWMSHE) approach.

Wanget al. (2017) create a SEPIC using a half-bridge LLC resonant converter. This architecture lowers system costs while increasing dependability. Switching losses are minimised because the LLC resonant component retains soft switching characteristics. System bus voltage may be maintained low in high-power LED driving systems by carefully selecting characteristics. To validate theoretical analysis, certain tests with a 100-W prototype are carried out. The obtained power factor was as high as 0.99, & the efficiency is up to 92% at full load due to soft-switching operations.

V. Viswanathan and Jeevananthan Seenithangom (2018) suggested a SEPIC converter with high static gain & low switching voltage stress; moreover, the converter is employed for torque ripple. In BLDC drive, the authors employed a three-level NPC inverter. The suggested SEPIC converter is not used to increase power factor.

Zhang et al. (2019) designed and analysed the double-axis gadget (mechanical structure). The Finite Element Method was used to generate parameterized model (FEM). The static analysis was performed to determine the displacement and stress distributions, as well as the stress evaluation, which was performed under various operating

International Journal on Recent and Innovation Trends in Computing and Communication
ISSN: 2321-8169 Volume: 11 Issue: 7
***Article Received:** 12 May 2023 **Revised:** 22 June 2023 **Accepted:** 20 July 2023*

situations. The start-up of fulfilling the stress intensity, the lightweight, was completed, and this served as the foundation for the device's prototype test. This study covers improved design working procedures that were carried out using a mathematical model, generated the Finite Element Model (FEM), applied the boundary conditions, and calculated and evaluated the stress. The prototype model's tracking precision is a bit greater, and the full load of the moving structure is in two key locations, which may lead to failure at times.

Lim and colleagues (2020) developed a large-scale dual-axis solar monitoring system that incorporates many row elevation structures as well as a vertical-axis rotating platform. The installation has a power of 60 kWp, a diameter of 35 m, and a transmission system that turns the whole rotating platform. The transmission mechanism is made up of an ACmotor (750 WAC) with a gearbox, 22 DC motors (15 WDC) for elevation motions, cylindrical pins, & a double layer pin-gear, all of which are unique design concepts that have been applied in a large-scale dual axis tracking system. The energy converter does away with the need for a diode bridge rectifier at the front end. Because the switches share the PWM gating signal, there is no need for additional circuitry to detect positive or negative ac input. The author created a 650-W prototype with a switching frequency of 70 kHz and a 400-volt alternating current output voltage.

William Cai et al. (2021) provide a summary of current research and technological advances in electric motor systems & electric power trains for new energy vehicles. Permanent magnet synchronous motors offer improved overall performance when compared to converters with Si-based IGBTs; converters with SiC MOSFETs have much higher efficiency & enhance driving mileage per charge when compared to converters with Si-based IGBTs. Moreover, the benefits and drawbacks of various control methods and algorithms are discussed. Finally, a technological roadmap for the next 15 years is offered, including the critical materials and components for the traction motor, power electronic converter, & electric power train for each time frame.

T M Khalina (2022) investigate a novel semiconductor device for starting a 3-phase induction motor from a single-phase network. Researchers were able to analyse the electromechanical properties of an induction motor when powered by a single-phase network using device simulation model created in Matlab Simulink environment. The parameters of motor during operation are compared using a 3-phase & a single-phase network. The investigation's findings indicate that developed gadget may be used to start & run a squirrelcage induction motor from a single-phase network. Simultaneously, engine's energy characteristics change somewhat.

OPERATION OF INDUCTION MOTOR DRIVE SYSTEM

An induction motor is an alternating current motor that works on the principle of electromagnetic induction. Because of their durability and brushless nature, they are commonly utilised in industrial drives. The squirrel cage induction motor is the most common form of electrical motor used in industry. The squirrel cage motor has many advantages, including.

1. Simple and tough construction. This translates to a low starting cost and great dependability for the consumer.
2. The combination of high efficiency and low maintenance costs leads in lower total operating expenses.

Squirrel cage motors speed depends upon various factors like applied frequency, pole pair number, and load torque. To reverse the machine's direction of rotation, the phase sequence to the motor must be changed. Their speed can be controlled with a variable frequency drive.

For adjustable speed applications, the induction machine, particularly the cage rotor type, is most commonly used in industry. In squirrel cage induction motors the rotor has squirrel cage like structure with shorted end rings and the stator has three-phase winding distributed sinusoidal. When ac voltages are applied to the three-phase stator winding it creates a magnetic field rotating at angular speed

$$\omega s = 4\pi fs/P$$

where f_s is the supply frequency in H_z and P is the number of stator poles.

When the rotor rotates at an angular speed of ω_r the conductors are subjected to a sweeping magnetic field, both voltage and current and mmf in the short-circuited rotor at a frequency $(\omega_s - \omega_r)P/4\pi$, known as the slip speed.

The interaction of air gap flux and rotor mmf produces torque. The per unit slip ω is defined as

$$S = \frac{\omega_{S-\omega_r}}{\omega_S}$$

Figure 1 shows the torque-speed curve. The various operating zones in the figure can be defined as plugging (1.0 < S< 2.0), motoring (0 < S< 1.0), and regenerating (S< 0). During normal motoring region, Te= 0 and S= 0, and as S increases Te also increases as a quasi-linear curve until breakdown, or maximum torque Tem is reached, Te decreases with the increase in S beyond this point.

International Journal on Recent and Innovation Trends in Computing and Communication
ISSN: 2321-8169 Volume: 11 Issue: 7
Article Received: *12 May 2023* ***Revised:*** *22 June 2023* ***Accepted:*** *20 July 2023*

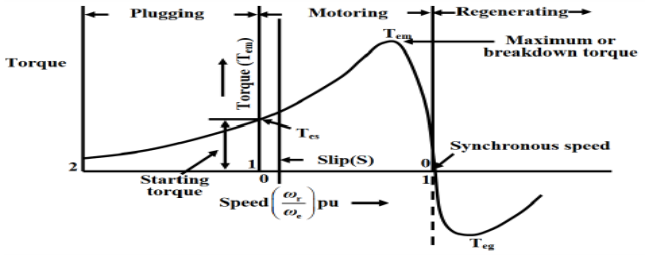

FIGURE 1: TORQUE-SPEED CURVE OF INDUCTION MOTOR

As the name implies, the machine functions as a generator in the regenerative zone. The rotor travels at super synchronous speed in the same direction as the air gap flux, resulting in negative slip and negative or regenerating torque (Teg). Variable-frequency control aids in adjusting the machine stator frequency in order to reduce the rotor speed (ωe<ωr) and achieve regenerative braking. Figure 1 shows the torque speed characteristics. It can be observed that the magnitude and/or frequency of the supply voltage may be changed at any rotor speed to get the appropriate torque.

An input Rectifier unit, an inverter unit, and a DC bus compose the Variable Frequency Drive. The supply voltage is linked to a rectifier unit, which receives AC power, and the three phase supply is supplied into a three phase full wave rectifier, which converts it to DC power. The DC bus has a filter element that filters out harmonics created during the AC to DC conversion. The last portion is an inverter section that includes six IGBTs (Insulated Gate Bipolar Transistors) that convert the filtered DC supply to a quasi sinusoidal wave of AC power that is linked to the induction motor. The input AC power is converted to DC, filtered, and then transformed to variable frequency DC by an inverter in a simple DC-link variable frequency motor controller. Because the synchronous speed of a motor is directly proportional to the supply frequency, the synchronous speed of the motor may be simply varied by adjusting the frequency value. This is the VFD's primary functioning phenomena.

BOOST CONVERTER WITH COMPOUND ACTIVE CLAMPING IN FOUR SWITCH THREE PHASE INVERTER FED INDUCTION MOTOR

The performance of a four switches three phase inverter (FSTPI) supplied induction motor with boost converter combined with compound active clamping is investigated in this chapter. The suggested converter is executed on a single phase supply, and its performance in terms of power factor, THD, and efficiency are evaluated. The active clamping branch of a converter is self-possessed by a clamping capacitor and an active switch connected in parallel with the resonant inductor. A voltage loop is formed in the circuit by the main switch, auxiliary switch, clamping capacitor, boost diode, and output filter capacitor. During switching periods, the converter switching devices are expected to be in the ON state. As a result of clamping the voltage across the switch in the off state, a parasitic oscillation between the junction capacitance of the boost diode and the resonant inductor is removed.

COMPOUND ACTIVE CLAMPING (CAC) BOOST CONVERTER

Figure 2 depicts the CAC boost converter circuit. The boost converter circuit uses a bridge rectifier to rectify the alternating current source, two inductors L1 and L2, and two switches S1 and S3. L1 is a boost inductor; L2 and CC are utilised for soft switching S3 with a set duty cycle. The duty cycle of main switch S1 varies with the input voltage and is adjusted to get the desired output voltage. When S1 is activated, inductor L1 is energised, and when S1 is deactivated, the energy stored in L1 is supplied to the capacitor C0.

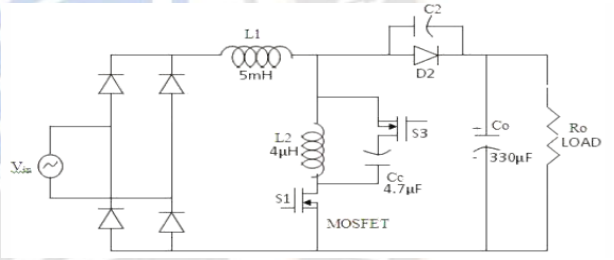

FIGURE 2: CAC BOOST CONVERTER CIRCUIT

The bridge rectifier is coupled via inductors L1, L2, and switch S1. When switch S1 is turned on, inductors L1 and L2 store energy, and switch S3, which is linked in parallel with inductor L2, operates as an auxiliary switch. Switch S1 is turned off in the next stage, and voltage across L2 appears across the load. Capacitors Cc and C0 are connected to switches S1 and S3, respectively, while capacitor C2 is connected to boost diode D2.

The input filter inductor L1 is selected to be very big so that the current iL does not change, allowing it to be regarded as a constant current source. When CC is high enough to eliminate voltage ripple, the filter capacitor CO can be represented as constant voltage sources. To a large degree, the resonant frequency of CC and L2 is lower than the working frequency of the converter. The suggested converter's main switch S1 and auxiliary switch S3 do not work in complimentary mode.

To clamp the voltage between main switch S1 and diode D2, auxiliary switch S3 is turned off for a brief period of time when both main switch S1 and diode D2 are

International Journal on Recent and Innovation Trends in Computing and Communication
ISSN: 2321-8169 Volume: 11 Issue: 7
***Article Received:** 12 May 2023 **Revised:** 22 June 2023 **Accepted:** 20 July 2023*

commutating circuits; hence, the duty cycle of auxiliary switch S3 is fixed while the duty cycle of main switch S1 varies with input voltage.

SIMULATION RESULTS

The boost diode is conducting prior to the initial stage, auxiliary switch S3 is switched off, and the current in L1 charges C3 paralleled and C1 paralleled with the main switch S1 discharges. At first, the voltage across S1 falls to zero, and the diode of S1 begins to conduct. Then, under zero voltage, S1 is switched on. The voltage across S3 is held constant at Vo +Vcc. The current in D2 is falling at this stage, whereas the current in S1 is growing at the same pace as D2. The resonant inductor L1 determines the current changing rate.

Figure 3 depicts an FSTPI-fed induction motor circuit with a boost converter and compound active clamping. The boost inductor is inductor L1. S2 is soft switched using inductors L2 and Cc. S1's duty cycle is modified to provide the needed DC voltage at the inverter's three phase four switch input. When S1 is activated, the energy in the inductor L1 is stored, and when S1 is deactivated, the energy in the inductor is provided to the capacitor Co. Switch S2 works as an auxiliary switch when connected in parallel with the inductor. This eliminates resonance between L1 and the diode's internal capacitance D5.

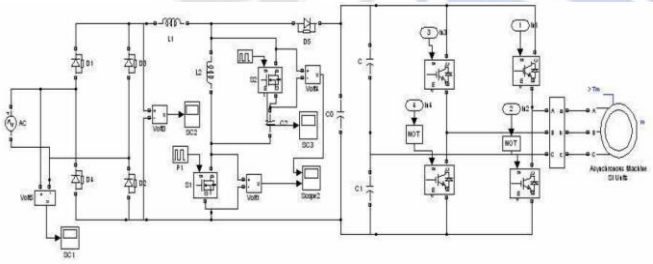

FIGURE 3 FOUR SWITCH THREE PHASE INVERTER FED INDUCTION MOTOR SYSTEM WITH COMPOUND ACTIVE CLAMPING

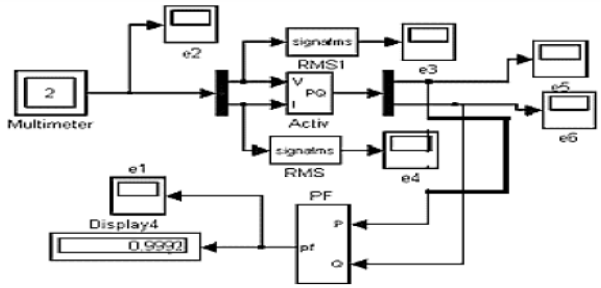

FIGURE 4: POWER FACTOR MEASUREMENT OF BOOST CONVERTER WITH COMPOUND ACTIVE CLAMPING

The power factor measuring circuit of a boost PFC converter is seen in Figure 4. When compared to the power factor of 0.990 (without active clamping) for the present soft switched PFC boost converter, the power factor attained is 0.999 (with compound active clamping). The power factor is enhanced by clamping the maximum voltage across the primary switch, and voltage ringing across the diode is eliminated. The switching pulses delivered to switches M1 and M2 are depicted in Figure 5. The phase voltage delivered to the three-phase induction motor is seen in Figure 6.

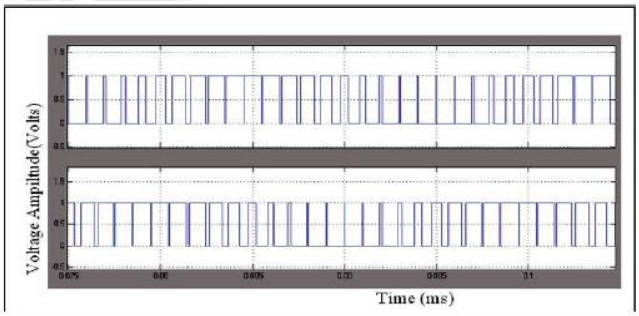

FIGURE 5: DRIVING PULSES FOR INVERTER

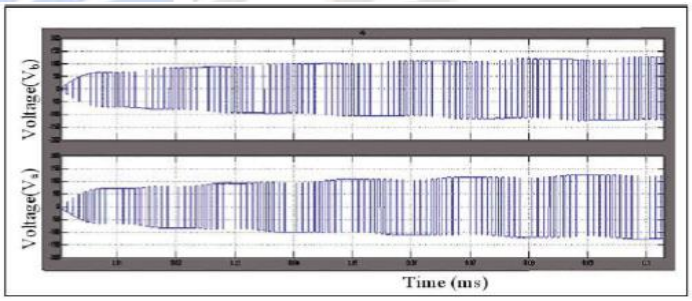

FIGURE 6: PHASE VOLTAGE OF INVERTER

Figure 7: depicts the efficiency of a three-phase induction motor with a boost converter and compound active clamping FSTPI. It is clear that the efficiency has increased to 95%. Switching losses are decreased in the proposed converter due to the use of a simple active snubber circuit, which provides zero voltage switching conditions for all switches. Because of the decreased number of components, it is more efficient and ideal for practical applications such as AC drive systems, power factor correction, UPS, and induction heating. As shown in Figure 8, the performance of the developed converter outperforms that of the current PFC boost converter.

International Journal on Recent and Innovation Trends in Computing and Communication
ISSN: 2321-8169 Volume: 11 Issue: 7
Article Received: *12 May 2023* ***Revised:*** *22 June 2023* ***Accepted:*** *20 July 2023*

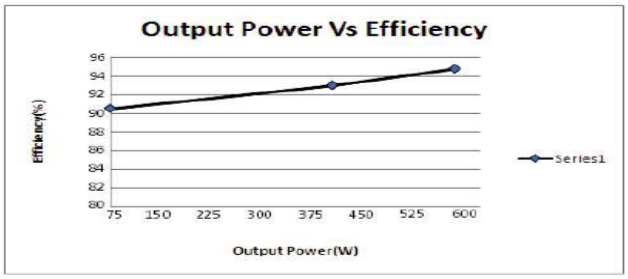

FIGURE 7: OUTPUT POWER VS EFFICIENCY OF BOOST CONVERTER WITH COMPOUND ACTIVE CLAMPING FSTPI FED INDUCTION MOTOR

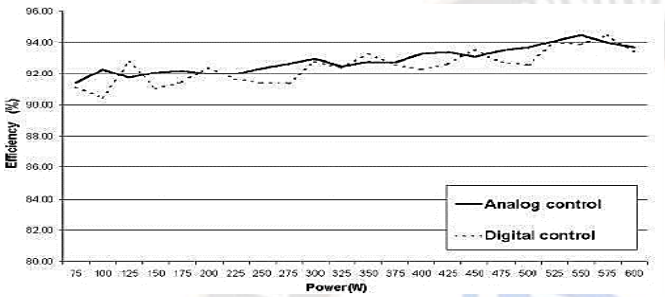

FIGURE 8: OUTPUT POWER VS EFFICIENCY OF SOFT SWITCHED PFC BOOST CONVERTER

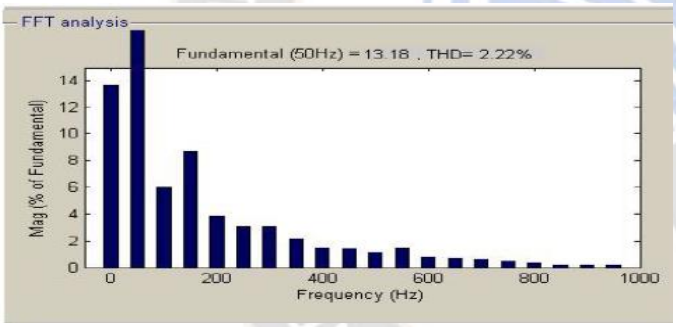

FIGURE 9: THD OF INPUT CURRENT FOR BOOST CONVERTER WITH COMPOUND ACTIVE CLAMPING FSTPI FED INDUCTION MOTOR

Figure 9 depicts the FFT analysis for the current of a boost converter with a compound active clamping FSTPI supplied induction motor. THD is decreased to 2.22% compared to 4.85% in the case of the previous soft switched PFC boost converter built by Luiz Henrique Silva Colado Barreto (2005). Table 1 compares the performance of a planned converter to that of an existing CAC converter.

TABLE 1: PERFORMANCE COMPARISON BETWEEN EXISTING CONVERTER AND PROPOSED CAC CONVERTER

PARAMETER	PERFORMANCE OF EXISTING	PERFORMANCE OF PROPOSED CAC
	CONVERTER	**CONVERTER**
Efficiency	92%	94%
Power Factor	0.94	0.998
THD	4.85%	2.22%

CONCLUSION

In this paper, the induction motor and BLDC motor drives were examined using boost converters, which were simulated and implemented in hardware prototypes. Matlab/simulink was used to model the boost converter with compound active clamping and FSTPI fed induction motor driving. To reduce the resonance in winding inductance and junction capacitance, the boost converter with compound active clamping supplied IM drive requires an extra diode and inductor. The planned converter was executed with an FSTPI fed induction motor, and results were obtained.

REFERENCES

1. Rahimi, A.M. and Emadi, A. Discontinuous-conduction mode DC/DC converters feeding constant-power loads‖, IEEE Transactions on Industrial Electronics, Vol.57, No.4, pp.1318-1329, 2010.
2. Rockhill, A.A., Liserre, M., Teodorescu, R. and Rodriguez, P. Gridfilter design for a multimegawatt medium-voltage voltage-source inverter‖, IEEE Transactions on Industrial Electronics, Vol.58, No.4, pp.1205-1217, 2011.
3. Errabelli, R.R. and Mutschler, P. ―Fault-tolerant voltage source inverter for permanent magnet drives‖, IEEE Transactions on Power Electronics, Vol.27, No.2, pp.500-508, 2012.
4. Lodhi, R & Thakur, P 2013, 'Performance & Comparison Analysis of Indirect Vector Control of Three Phase Induction Motor', International Journal of Emerging Technology and Advanced Engineering, vol.3,no.10, pp. 716-724.
5. Behera, P, Manoj Kumar Behera & Amit Kumar, S 2014,'Comparative Analysis of scalar & vector control of Induction motor through Modeling& Simulation', International Journal of Innovative Research in Electrical, Electronics, Instrumentation and Control Engineering, vol. 2, no. 4.pp.1340-1344.
6. Ashmore, E ' Modular solar support assembly', U.S Patent No. 9134045. 15 Sep. 2015.
7. Alexander S. Maklakov et al. (2016) "Power factor correction and minimization THD in industrial grid via reversible medium voltage AC drives based on 3L-NPC AFE rectifiers" DOI:

10.1109/IECON.2016.7793315 https://ieeexplore.ieee.org/abstract/document/7793315.

8. Viswanathan, V. and Seenithangom, J., 2018. Commutation Torque Ripple Reduction in the BLDC Motor Using Modified SEPIC and Three-Level NPC Inverter. IEEE Transactions On Power Electronics, vol. 33 no.1, pp.535-546.
9. Zhang, S. Li, C, Zhang, J, Miao, H & Zhang, Y 2019, 'Design and structural analysis of the Sun ray double axis tracking device', Journal of Solar Energy Engineering, vol. 141, ho. 4.
10. William Cai et al. (2021) "Review and Development of Electric Motor Systems and Electric Powertrains for New Energy Vehicles" Published: 25 February 2021 valum 4, pages3–22.
11. T M Khalina et al. (2022) "The development of an energy efficient electric drive for agricultural machines" Volume 1211, IXX International Scientific and Practical DOI 10.1088/1757-899X/1211/1/012018.
12. Lim and colleagues (2020) "Grid-Connected Photovoltaic Systems with Single-Axis Sun Tracker: Case Study for Central Vietnam" Volume 13 Issue 6 10.3390/en13061457.https://www.mdpi.com/1996-1073/13/6/1457.